SPENT FUEL DRY STORAGE CASK THERMAL MODELING ROUND ROBIN

A. CSONTOS, K. WALDROP
Electric Power Research Institute
3420 Hillview Avenue, Palo Alto, CA 94304, USA

S. DURBIN
Sandia National Laboratories
P.O. Box 5800, Albuquerque, NM 87123, USA

B. HANSON
Pacific Northwest National Laboratory
902 Battelle Blvd, Richland, WA 99354, USA

J. BROUSSARD, G. LENCI
Dominion Engineering, Inc.
12100 Sunrise Valley Dr, Reston, VA 20191, USA

ABSTRACT

Thermal analyses of dry storage systems for spent nuclear fuel conducted using subchannel analysis or computational fluid dynamics adopt design basis assumptions and inputs to ensure the peak cladding temperature does not exceed an established limit. Consequently, a best-estimate understanding of the thermal behaviour of the system that includes accurately quantified uncertainties is not available from those models. This work presents the results of a double-blind benchmark aimed at assessing the accuracy of dry storage system simulations and gaining insight on the main causes of modelling uncertainty. A total of four submissions to this round robin are compared with experimental data acquired by the DOE/EPRI High Burnup (HBU) project. In the configuration used, 32 HBU pressurized water reactor assemblies are stored in a bolted cask with thermocouples inside the fuel recording internal temperatures. Results highlight the importance of developing a refined assessment of key uncertainty terms in modelling solutions, especially those related to internal gap size variations.

1. Introduction

Vendors of dry storage systems for used nuclear fuel typically design and license casks and canisters using thermal analyses supported by numerical simulations [1]. One key result from these simulations is the peak cladding temperature (PCT) predicted for the system design. Typically, bounding assumptions and engineering margins are used in the simulations to account for uncertainties in the analysis methodology and ensure that regulatory limits are not exceeded. These bounding assumptions, in turn, can lead to underutilized storage capacity for system designs, resulting in longer fuel cooling times in used fuel pools. Additionally, bounding approaches for PCT values tend to also predict elevated external system wall temperatures, resulting in potentially non-conservative estimates for chloride-induced stress corrosion cracking susceptibility from deliquescence [2]. To overcome this limitation, vendors typically develop additional thermal models to provide conservative inputs for estimating chloride-induced stress corrosion cracking [3]. Quantifying the uncertainty and reducing the resulting bounding assumptions in thermal simulations will lead to more efficient storage and ultimate disposal of used fuel.

Research results on best-estimate model development are documented in the literature and have used computational fluid dynamics (CFD) or subchannel analysis codes [4,5,6].

Supporting the effort to develop and improve best-estimate models, a thermal modelling program was established by U.S.-based collaborating entities including the U.S. Department of Energy (DOE), U.S. National Laboratories, the Electric Power Research Institute (EPRI), the U.S. Nuclear Regulatory Commission (NRC), research institutions, vendors, and utilities. A first phase of the program was completed in the NRC/DOE Boiling Water Reactor (BWR) Dry Cask Simulator project [7]. The project acquired temperature data inside an instrumented and electrically-heated prototypic BWR test assembly placed into a storage basket and a cylindrical pressure vessel. The experimental data were collected with the purpose of enabling CFD model validation.

This report describes a second phase of the thermal modelling program, in which a round robin led by EPRI was performed on a conductive dry storage system, aiming at assessing model uncertainties and ultimately increasing the accuracy of thermal simulation approaches. This report documents the results of a double-blind benchmark study comparing measured temperature data, acquired from a dry storage system loaded with used nuclear fuel, to modelling temperature predictions. Round robins are useful tools to evaluate the reliability of models in complex applications [8]. Because the benchmark is double-blind, no data are exchanged between modelers and measurement results except for official inputs, allowing evaluations of modelling uncertainty while excluding the potential for confirmation bias. The measurement data were obtained from the DOE/EPRI High Burnup (HBU) project and used a TN-32B dry storage system instrumented with thermocouples and loaded with used pressurized water reactor (PWR) fuel at the North Anna Power Station.

The next section describes the configuration of the HBU project system and provides an overview of benchmark input data. Then, benchmark submissions are briefly described, and results are compared with measurement data. Observations are finally made on results, commenting on the observed positive offset of modelled internal temperature with respect to measured data.

2. Benchmark description

In the HBU project, a TN-32B dry storage system was loaded with high-burnup used nuclear fuel at the North Anna Power Station. The system was instrumented with internal thermocouples placed inside a guide tube in each of 7 fuel assemblies selected out of the total 32 assemblies loaded in the system. Custom lances were used to insert 9 K-type thermocouples per each guide tube (9×7 = 63 total thermocouples) while maintaining a pre-determined axial spacing between them. Instrumentation was inserted using 7 custom penetrations drilled into the system's lid as shown in Fig. 1. Lead blankets were placed over the holes on the closed lid for radiation shielding.

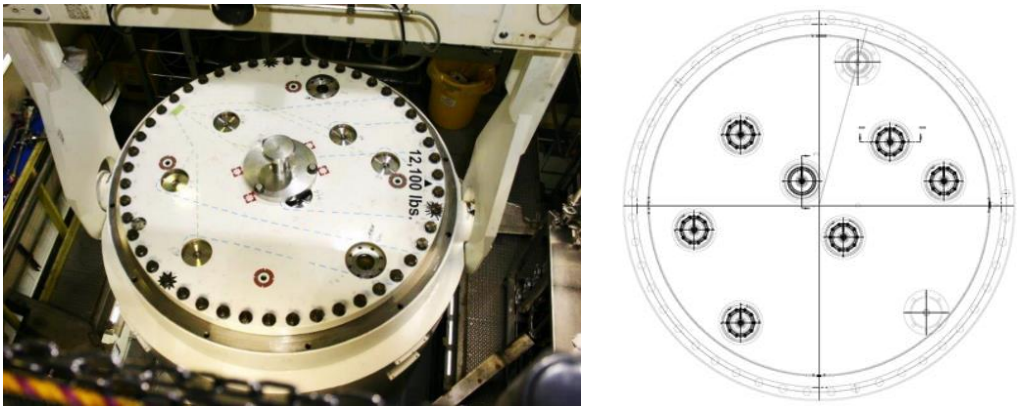

Fig. 1 Modification to the lid to allow for the insertion of 7 thermocouple lances. The left picture is courtesy of Dominion Energy.

In addition to the internal measurements, external temperature acquisitions were performed on the external surface using an infrared (IR) gun. To acquire readings, the gun was pointed at pre-determined marks that were made on the surface. Those locations are distributed over a 3×5 array, as illustrated in Fig. 2a.

a)

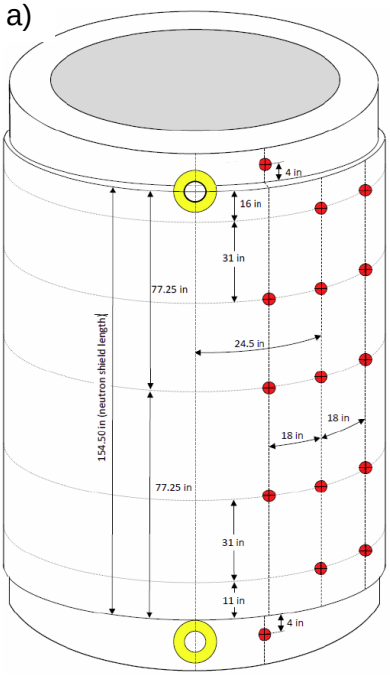

b)

	1 6T0 NAIF/P+Z Zirlo, 54.2 GWd 4.25%/3 cy/12.1 yr 912.2 W	2 (TC Lance) 3K7 AMBW M5, 53.4 GWd 4.55%/3 cy/8.7 yr 978.2 W	3 3T6 NAIF/P+Z Zirlo, 54.3 GWd 4.25%/3 cy/12.1 yr 914.4 W	4 6F2 NAIF/P+Z Zirlo, 51.9 GWd 4.25%/3 cy/13.5 yr 799.5 W	Drain Port
5 3F6 NAIF/P+Z Zirlo, 52.1 GWd 4.25%/3 cy/13.5 yr 800.9 W	6 (TC Lance) 30A AMBW M5, 52.0 GWd 4.55%/3 cy/7.2 yr 1008.6 W	7 22B AMBW M5, 51.2 GWd 4.55%/3 cy/5.7 yr 1142.4 W	8 (PRA) 20B AMBW M5, 50.5 GWd 4.55%/3 cy/5.7 yr 1121.2 W	9 5K6 AMBW M5, 53.3 GWd 4.55%/3 cy/8.7 yr 975.1 W	10 5D5 NAIF/P+Z Zirlo, 55.5 GWd 4.20%/3 cy/17.7 yr 814.5 W
11 (Vent Port) 5D9 NAIF/P+Z Zirlo, 54.6 GWd 4.20%/3 cy/17.7 yr 802.6 W	12 28B AMBW M5, 51.0 GWd 4.55%/3 cy/5.7 yr 1135.0 W	13 (PRA) F40 LOPAR Zry-4, 50.6 GWd 3.59%/3 cy/30.6 yr 573.8 W	14 (TC Lance) 57A AMBW M5, 52.2GWd 4.55%/3 cy/7.2 yr 1037.0 W	15 (PRA) 30B AMBW M5, 50.6 GWd 4.55%/3 cy/5.7 yr 1124.8 W	16 3K4 AMBW M5, 51.8 GWd 4.55%/3 cy/8.7 yr 941.3 W
17 5K7 AMBW M5, 53.3 GWd 4.55%/3 cy/8.7 yr 961.7 W	18 (PRA) 50B AMBW M5, 50.9 GWd 4.55%/3 cy/5.7 yr 1131.1 W	19 (TC Lance) 3U9 NAIF/P+Z Zirlo, 53.1 GWd 4.45%/3 cy/10.6 yr 920.2 W	20 (PRA) 0A4 NAIF Low-Sn Zry-4, 50.0 GWd 4.00%/2 cy/23.2 yr 646.2 W	21 15B AMBW M5, 51.0 GWd 4.55%/3 cy/5.7 yr 1135.8 W	22 6K4 AMBW M5, 51.9 GWd 4.55%/3 cy/8.7 yr 941.2 W
23 3T2 NAIF/P+Z Zirlo, 55.1 GWd 4.25%/3 cy/12.1 yr 934.7 W	24 (TC Lance) 3U4 NAIF/P+Z Zirlo, 52.9 GWd 4.45%/3 cy/10.6 yr 914.2 W	25 (PRA) 56B AMBW M5, 51.0 GWd 4.55%/3 cy/5.7 yr 1133.7 W	26 54B AMBW M5, 51.3 GWd 4.55%/3 cy/5.7 yr 1136.3 W	27 6V0 AMBW M5, 53.5 GWd 4.40%/3 cy/8.7 yr 988.2 W	28 (TC Lance) 3U6 NAIF/P+Z Zirlo, 53.0 GWd 4.45%/3 cy/10.6 yr 916.9 W
	29 4V4 AMBW M5, 51.2 GWd 4.40%/3 cy/9.1 yr 914.2 W	30 5K1 AMBW M5, 53.0 GWd 4.55%/3 cy/8.7 yr 968.0 W	31 (TC Lance) 5T9 NAIF/P+Z Zirlo, 54.9 GWd 4.25%/3 cy/12.1 yr 927.7 W	32 4F1 NAIF/P+Z Zirlo, 52.3 GWd 4.25%/3 cy/13.5 yr 804.3 W	

Fig. 2 a) External temperature reading positions; b) cask loading map

The internal and external temperature readings are the focus of this benchmark. Temperature measurements were made during system draining, drying, and storage, but the benchmark only focuses on the last part, i.e., storage in a decontamination pit at the plant site. The modelers and the measurement vendor evaluated the temperatures independently and submitted their results to EPRI around the same date for analysis to ensure the validity of the double-blind approach. Measurements were recorded for about 13 days, during which temperature readings were confirmed to reach a statistically stationary behaviour, justifying steady-state numerical modelling.

As part of the round-robin problem statement, modelers were asked to use the proprietary geometry of the TN-32B system and were provided information about the surrounding environment and loaded fuel, including the external temperature. Modelers were asked to all use the same inputs, although model assumptions and methods could vary. Using the same inputs allows separation of model uncertainty from input sensitivity. Sensitivity was analysed by previous studies [6,9] which concluded that model results are strongly sensitive to decay heat, external temperature, and internal gaps. The first two parameters have been provided precisely to modelers as part of the input information. However, internal gap sizes were generally taken from the final safety analysis report (FSAR) design basis model and tended to predict higher temperatures (open gaps rather than closed). Additional evaluation of the gap condition uncertainty has been performed after completion of the round robin study; these results are likely to be presented and/or published separately by individual modelers.

Ambient temperature was measured with thermocouples and determined to be 23.9 °C by averaging the measured temperature history. The ambient temperature had a day-night fluctuation range of about ±6 °C. Decay heat input data were provided in the form of a per-

assembly power and a general axial distribution curve. Both inputs were determined using a best-estimate, highly accurate method developed by the Oak Ridge National Laboratory. The original design basis heat load for the system was calculated as 36.96 kW, which was then refined to 32.934 kW for an amended license. The 32.934 kW heat load is about 8% higher than the 30.456 kW heat load developed for the round robin inputs. The system was loaded with 32 PWR assemblies each with 17 x 17 rods and high-burnup fuel. The assembly types are based on different Westinghouse or AREVA designs, specifically: LOPAR, NAIF, NAIF/P+Z, and AMBW. Relevant non-proprietary features of those fuel assemblies were provided to modelers. A loading map of the assemblies inside the dry storage system was also given to the modelers as shown in Fig. 2b. The map contains relevant details such as: assembly identifier, fuel type, cladding material, average burnup, initial enrichment, number of irradiation cycles, years since reactor discharge as of 11/7/2017, and decay heat. The loading map also marks the presence of a thermocouple lance or poison rods (indicated as "poison rod assembly", PRA) in some of the assemblies.

3. Submissions

The benchmark received 4 submissions of simulation results from 3 different organizations. The submissions are identified using anonymous labels S1 through S4, as shown in Tab. 1.

Tab. 1 Summary of submissions

Submission	Method	Software
S1	Finite volume CFD	ANSYS Fluent
S2	Finite volume CFD	STAR-CCM+
S3	Subchannel	COBRA-SFS
S4	Thermal finite element analysis	ANSYS APDL

As noted in Tab. 1, model results were obtained using 3 different solution methods, i.e., finite volume CFD, thermal finite element analysis (FEA), and subchannel analysis, and all different pieces of software. Such a variety of simulation tools supports an evaluation of modelling error being free from code-specific or method-specific considerations.

4. Results

4.1 Uncertainties

Plots presenting results in this work show error bars for the measured data values. The measurement uncertainty σ_{meas} is determined as the sum in quadrature of two values. The first is a sensor uncertainty, σ_{sen}, i.e. the measurement uncertainty at a known position. The second is a locational uncertainty, σ_{loc}, i.e. a measurement uncertainty component due to uncertainty about the location where the measurement is made.

$$\sigma_{\text{meas}} = \left(\sigma_{\text{sen}}^2 + \sigma_{\text{loc}}^2\right)^{1/2} \quad \text{Eq. 4-1}$$

For internal thermocouple readings, sensor uncertainty is determined using the ISO/IEC 98-3 standard as 1.4 °C plus 0.3 % of the measured value in °C, valid in the range of temperatures of this work with a 95 % confidence and a normal distribution. Locational uncertainty is determined using a range of ±1/4 inches to account for uncertainty in the position of TCs in the lance and of the lance in the guide tube. This spatial uncertainty is multiplied by the local average axial temperature gradient.

For external IR gun measurements, sensor uncertainty is determined from the IR gun user manual, which, in the temperature range of interest in this work, specifies a fixed value of 2 °F (1.1 °C). Locational uncertainty relates to the finite size of the circles on which the IR gun was pointed. By inspection of Fig. 2a along with dry cask pictures, the spatial uncertainty due to circle size is estimated as ±3/8 inches. This spatial uncertainty is combined with axial temperature gradients using the same method adopted for internal temperatures.

Although data were measured for the 13 days of system residence in the decontamination pit at the plant, representative steady-state values for the last two days of system residence are presented here. Error bars for the measurement results do not include terms accounting for daily temperature fluctuations, which varied by less than 1°C in measured temperature over the two-day period considered.

Additionally, calculated uncertainty range values were provided with the submission S1 results. The values were calculated according to the ASME V&V 20 [10] approach and using a first-order sensitivity analysis. The uncertainty range values were received before the S1 modelers obtained the measured data, so they were produced in a blind fashion.

4.2 Internal temperature results

The benchmark comparisons between simulation results and measured data for internal temperature profiles are shown in Fig. 3. The figure compares thermocouple data and modeler submission predictions for three of the seven instrumented fuel assemblies. Results are presented both on a regular temperature scale and using temperature differences[1] with respect to measured data.

All modelling results predict quasi-parabolic temperature distributions replicating qualitatively the shapes observed in the measured data. However, 248 out of 252 submitted base-case simulation points predict greater temperatures than the measurements. About half of the error bars for submission S1 encompass experimental data.

Most of the base-case simulation data points exceed the measured data by about 20-100 °C. Observations can be made regarding plots showing deviations from the measurement data, as presented at the right of Fig. 3. A trend appears for the base case of submissions S1 and S4 showing a deviation from the measured values that increases almost linearly from the top to the bottom of the system, frequently reaching 50-95 °C of deviation between model results and measurements. The cause for this slope in deviation plots is most likely related to modelling details, e.g., geometry including internal gap sizes, fluid mechanics treatments, and boundary conditions. It is also noted that the results from submission S4 are in most cases higher by at least 25 °C with respect to those from the other modelers. This offset will be discussed in Section 4.3 by observing trends in external temperatures.

Overall, deviations between base-case modelling results and measured data are all much greater than the measurement error bars. A detailed analysis of daily temperature variations, which result in a measured range of less than 1 °C as discussed in Section 4.1, would not justify the observed deviation, which exceeds in most cases, 20 °C and is single-sided toward higher modelling values. The cause of this bias is mainly attributable to the model. In other words, using the nomenclature in Section 1 of ASME V&V 20 [10], the error in the model solution value is expected to be much larger than the experimental error.

[1]Deviation plots for both internal and external temperatures use error propagation to determine error bars. Measurement-deviation error bars are calculated as: $(2\sigma_{\mathrm{meas}}^2)^{1/2}$, while deviation error bars for S1 modelling results as: $(\sigma_{\mathrm{meas}}^2+\sigma_{\mathrm{s1}}^2)^{1/2}$.

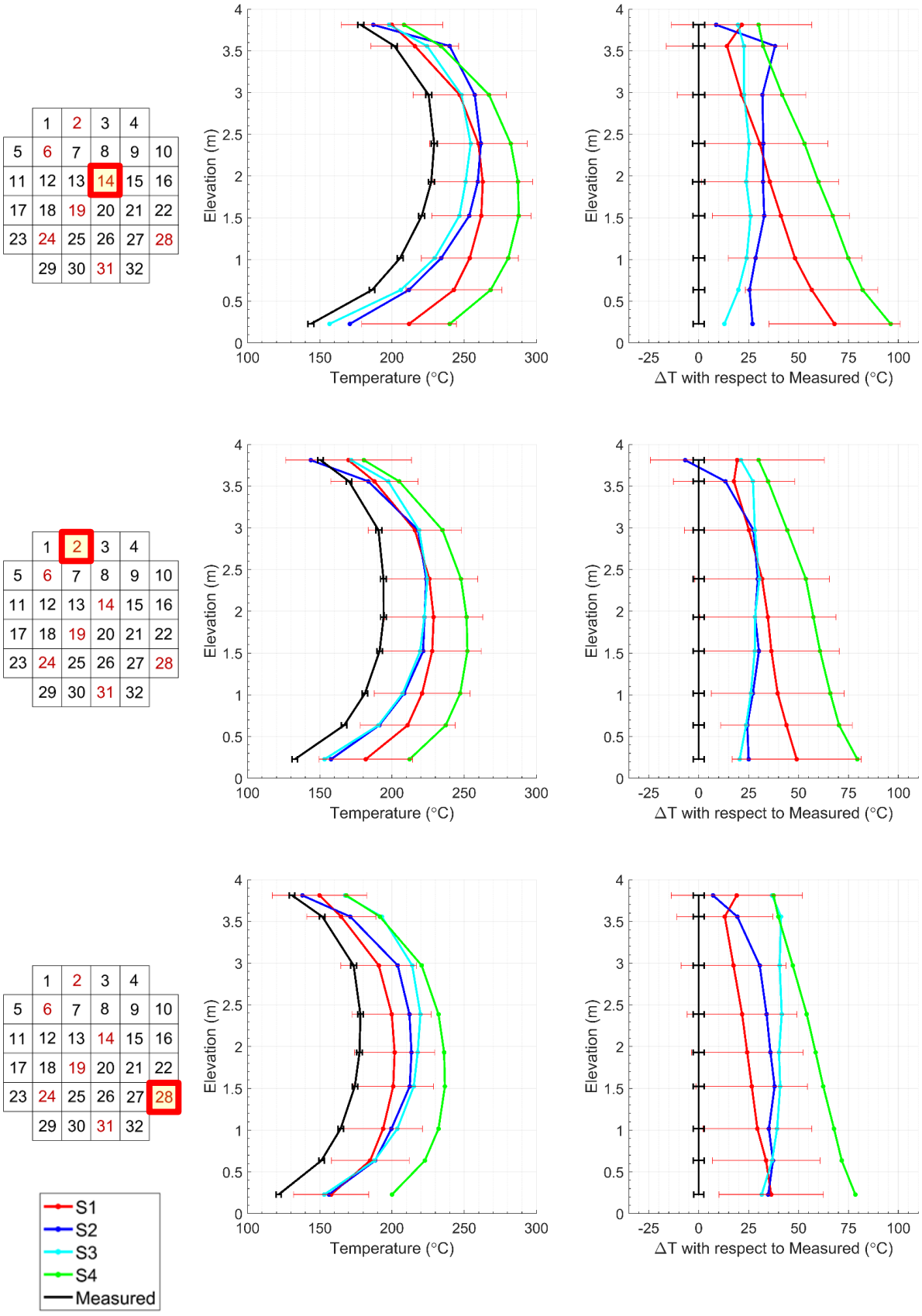

Fig. 3 Temperature results at positions of internal thermocouples for 3 example assemblies, namely number 14, 2, and 28.

4.3 External temperature results

Results for external temperatures are shown in Fig. 4. Similar to the approach used for internal temperature results, temperature scales are shown in plots in the left part of the figure and deviations from the measured data in the right part. Data are organized based on the 3 columns on the system's surface illustrated in Fig. 2a. S3 provided results without a circumferential variation and without data for the top and bottom points of the first column.

Most base-case data points for submissions S1 and S2 are very close to the measured data – in most cases within 5 °C, and S1 error bars encompass experimental uncertainty ranges. Results from S3 show slightly higher temperatures than S1 and S2, but still low deviations from measured data – in most cases smaller than 10 °C. On the other hand, submission S4 shows a significant positive offset from the measured data between about 20 and 48 °C.
A model description obtained from modeler S4 indicates that the deviation may derive from strongly conservative choices made in the treatment of heat transfer between the system's surface and the room. The positive offset for S4 has a magnitude similar to that observed for S4 in internal temperatures, pointing to a potential causality.

In principle, external temperatures can be determined with the sole knowledge of the ambient temperature, decay heat, heat distribution, and heat transfer coefficient. The accuracy of submissions S1 through S3, achieved without the strongly conservative assumptions of S4, conveys a substantial level of confidence about the accuracy of two key input parameters to which models are known to be very sensitive [6,9], i.e. decay heat and ambient temperature.

5. Conclusions and discussion

Results of a conductive dry storage system thermal modelling round robin are presented in this report, comparing four submitted best-estimate simulation results with measured temperature data from the DOE/EPRI HBU project. As the benchmark was double-blind, measurement data and model results have been submitted to a third party simultaneously. The four submitted modelling results were obtained using three different simulation methods (finite volume CFD, thermal finite element analysis, and subchannel analysis) and four different software packages (ANSYS FLUENT, STAR-CCM+, COBRA-SFS, and ANSYS-APDL). The diversity of approaches enables a comparison providing valuable information on modelling uncertainty. Although uncertainties in modelling results were not requested in the benchmark, one modeler, S1, has quantified and submitted those values along with the base-case results.

Modelling results and measured data for the system's external wall are generally consistent with each other, except for one submission, which used conservative assumptions for external boundary conditions. The similarity between model and measurement at this location provides confidence on the accuracy of benchmark inputs to which simulations are known to be sensitive, namely decay heat and ambient temperature. Uncertainty bars for S1 model results encompass the uncertainty range for external measured data.

On the other hand, internal temperature profiles in base-case model submissions show a positive offset by about 20-100 °C with respect to measured data, despite overall distributions resembling the data. An observed additional offset in submission S4 may be a result of the conservative external boundary conditions used by that submission. A slope in plots of temperature deviation is also observed for submissions S1 and S4 base cases with the error increasing from top to bottom. This slope is believed to derive from modelling treatments for boundary conditions and fluid mechanics. For internal temperatures, about half of the S1 uncertainty bars encompass the uncertainty range of measured data.

These observations on internal results, along with the high sensitivity of results to input data observed by modelers, lead to an appreciation of the importance of input uncertainty relative to physical model and numerical uncertainty.

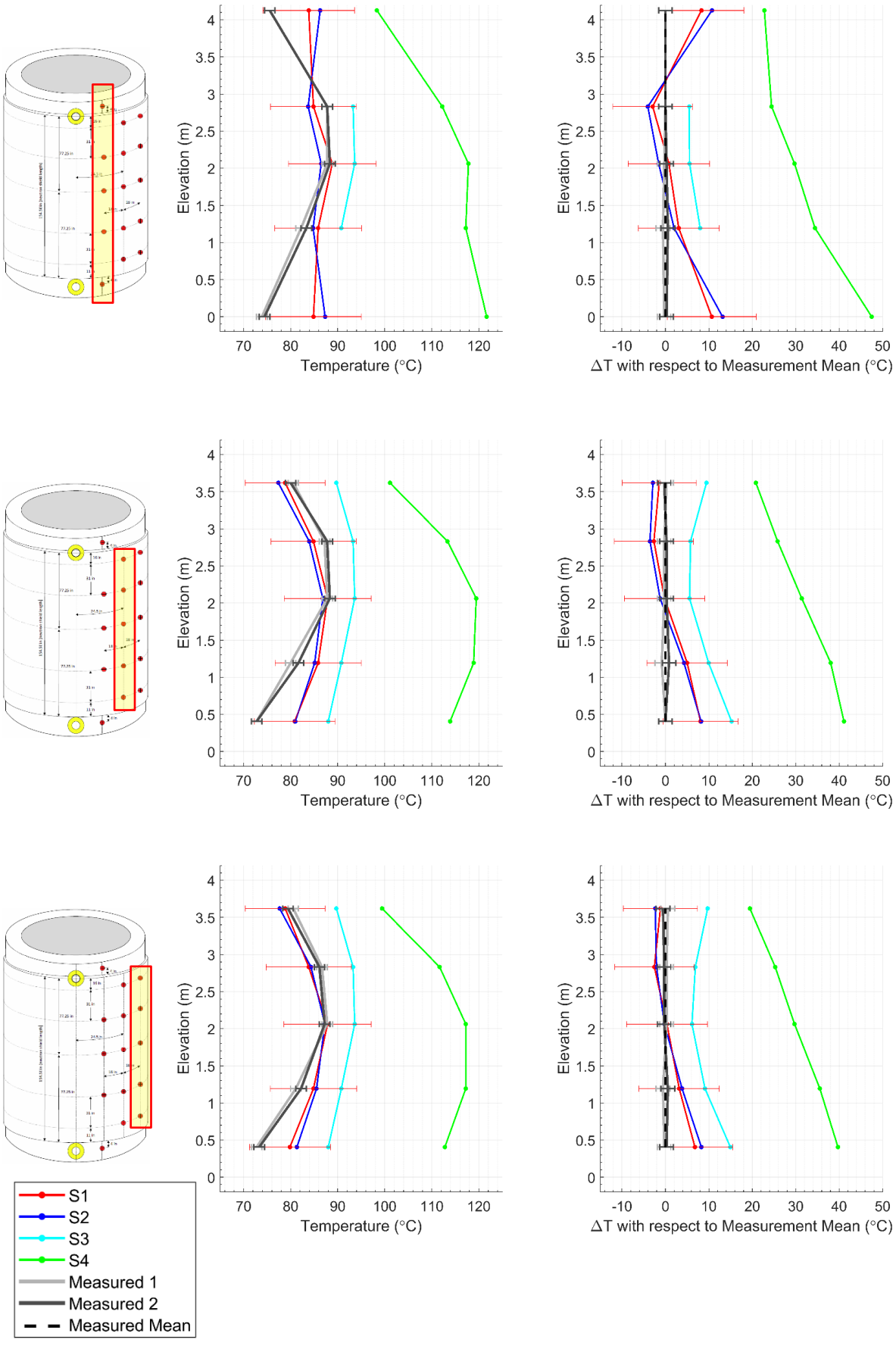

Fig. 4 Results at external thermocouple positions.

The observed offset of base-case results often appears to be much larger than the deviation between results from different models that did not use conservative external boundary conditions (i.e., S1, S2, and S3).

A preliminary analysis of the causes of the offset in internal temperature results suggests that among all sources of input sensitivity for the system considered in this exercise, the size of internal gaps inside the system might have been a major cause of deviation. In fact, a discussion with the modelers made after the release of results has highlighted that significant changes in thermal modelling results toward lower temperatures arise when one or more gaps are closed, which is a condition plausible to occur in multiple system locations simultaneously due to basket movement, thermal expansion, realistic conditions of gravity, etc. The gap condition and other uncertainty components could be assessed by future research that may follow along and refine the techniques that have been used by modeler S1 to determine the uncertainty in modelling results.

Overall, the benchmark has been successful in identifying useful paths to be followed by future work to develop accurate best-estimate models with uncertainty quantification. The exercise has confirmed that models used for system design and licensing, while conservative, result in positive deviations, for the internal temperature, of around 25-70 °C relative to measured values from the benchmark. Additionally, a positive deviation of about 90 °C was found between the 318 °C value for PCT calculated for the revised system licensing basis and the maximum measured internal temperatures (which generally correspond to PCT values).

After the success of the BWR and HBU projects, a third planned phase is envisioned that will use an instrumented next-generation cask to support further model advancement.

6. Acknowledgements

Multiple organizations have provided invaluable contributions supporting the thermal modelling round robin collaboration. Those organizations include, in addition to the authors' affiliations, the U.S. Department of Energy, Oak Ridge National Laboratory, Pacific Northwest National Laboratory, Sandia National Laboratories, the U.S. Nuclear Regulatory Commission, the Nuclear Energy Institute, Orano TN, and Dominion Energy.

7. References

1. U.S. Nuclear Regulatory Commission, Standard Review Plan for Spent Fuel Dry Storage Systems at a General License Facility, Final Report, NUREG-1536, Revision 1, July 2010.
2. X. He, T. Mintz, R. Pabalan, L. Miller, G. Oberson, Assessment of Stress Corrosion Cracking Susceptibility for Austenitic Stainless Steels Exposed to Atmospheric Chloride and Non-Chloride Salts, U.S. Nuclear Regulatory Commission Regulation, NUREG/CR-7170, Washington DC, USA, February 2014.
3. U.S. Nuclear Regulatory Commission Office of Nuclear Material Safety and Safeguards, Safety Evaluation Report for the Standardized NUHOMS® System, Certificate of Compliance No. 1004, Renewal Docket No. 72-1004, Revision 0, May 2017.
4. L.E. Herranz, J. Penalva, F. Feria, CFD analysis of a cask for spent fuel dry storage: Model fundamentals and sensitivity studies, Annals of Nuclear Energy 76, pp. 54–62, 2015.
5. J. Li, Y.Y. Liu, Thermal modeling of a vertical dry storage cask for used nuclear fuel, Nuclear Engineering and Design 301, pp. 74–88, 2016.
6. R.R. DeVoe, K.R. Robb, S.E.Skutnik, Sensitivity analysis for best-estimate thermal models of vertical dry cask storage systems, Nuclear Engineering and Design 320, pp. 282–297, 2017.

7. S.G. Durbin and E.R. Lindgren, Thermal-Hydraulic Results for the Boiling Water Reactor Dry Cask Simulator, Sandia National Laboratory Report, SAND2017-10551 R, Albuquerque NM, USA, September 29, 2017.
8. B.L. Smith, J.H. Mahaffy, K. Angele, J. Westin, Report of the OECD/NEA-Vattenfall T-Junction Benchmark exercise, Report NEA/CSNI/R(2011)5, 2011.
9. K. Robb, Thermal Modeling Sensitivities with COBRA-SFS for Vertical Dry Casks with Limited Internal Convection, American Nuclear Society Winter Meeting, Washington DC, November 8-12, 2015.
10. American Society of Mechanical Engineers, Standard for Verification and Validation in Computational Fluid Dynamics and Heat Transfer, ASME V&V 20-2009, 2009.
11. U.S. Nuclear Regulatory Commission Spent Fuel Project Office, Interim Staff Guidance 11, Revision 3, November 2003.